Bitlis Eren University
Journal of Science and Technology

ISSN 2146-7706
2, (2012), 44-48

Research Article

Molecular dynamics simulation of crystallization of amorphous aluminium modelled with EAM

Fatih Ahmet Çelik

Bitlis Eren University, Faculty of Arts and Science, Department of Physics, 13000, Bitlis, Turkey
Corresponding author: e-mail: facelik@beu.edu.tr

Abstract

The crystallization process of a amorphous aluminium (Al) containing 2048 atoms is studied with molecular dynamics (MD) simulation. Amorphous and crystal structure of Al is reproduced by applying fast cooling treatment and crystal behaviour from amorphous phase by means of MD simulation. The local order of the system have been analysed by bond orientational order parameters, the radial distribution functions and atomic coordinates. The simulation results also show that there are transformations from a disordered structure to a stable crystal phase during the crystallization.

Keywords: Molecular dynamics, embedded atom method, local order, nucleation

1. Introduction

Many systems, such as amorphous and polycrystalline solids are usually prepared by the process of solidification of the liquid phase. Glass or amorphous phase is considered to be frozen liquid and it means that various atomic clusters in liquid state do not have enough time to move their rearrangement of equilibrium to form crystalline under cooling conditions (Lu 1996; Desré et al. 2001; Schuh et al. 2007). Atomic clusters provide a bridge between atoms and molecules and bulk materials, therefore, they have been used in exploring the microstructures of liquid, amorphous and solid metals. In the past several years, the structural properties of small clusters have been studied by using a variety of techniques (Erkoc 1998; Proykova et al. 2006; Celik et al. 2008).

MD simulations based on the inter-atomic interactions are widely used on the studies of structural properties of metals or its alloys and amorphous systems. The embedded atom method (EAM) originally proposed by Daw & Baskes (1984) based on many body interactions has been used confidently in MD simulations for metallic systems and used widely to solve many problems in bulk, surface and interface of metals and alloys (Brown & Adams 1995). However, the EAM applications on the liquid and amorphous phases of metallic systems are also increasing from day to day (Pei et al. 2005; Kazanc 2007).

Bond orientational order parameters, which were determined by means of spherical harmonics have been used to determine the local symmetric properties of cluster in liquid or amorphous state (Nelson & Toner 1981). For example as, one of the earliest interesting studies, Steinhardt et al. (1983) to calculate bond-orientational order using molecular dynamics simulations of supercooled liquids and models for metallic glasses in three dimensions.

In this paper, we present the results obtained on the effect of crystallization on the local order and dynamics related to the slow cooling process.

In addition to this, structural analysis using bonding orientational order has been performed in detail and the effect of undercooling on the microstructure has been analyzed. The structure of the obtained liquid, amorphous and crystal phases has been analysed by using radial distribution function (RDF) and MD simulations are used to study the crystallization process of amorphous mono-atomic Al system. The essential technical details of the computational method used are given here, and the results have been discussed. Finally, our main conclusions have been summarized.

2. Interatomic potential

In the EAM formalism, the binding energy of atom *i* in a crystal with *N* atoms is a sum of contributions from the pair potential and embedding potential functions. Various approaches have been applied to define EAM functions (Wang & Dellago 2003).

In this approach the total crystal energy is calculated from:

$$E_T = \varepsilon \sum_{i=1}^{N} \left[\frac{1}{2} \sum_{j \neq i}^{N} \left(\frac{a}{r_{ij}} \right)^n - c\sqrt{\rho_i} \right] \quad (1)$$

$$\rho_i = \sum_{j \neq i}^{N} \left(\frac{a}{r_{ij}} \right)^m \quad (2)$$

Here, *rij* is the distance between atoms *i* and *j*, c is a positive dimensionless parameter, ε is a parameter in dimension of energy, a is the lattice constant, and m and n are positive integers, which are determined by fitting to the experimental properties of material such as lattice constant (a), cohesive energy (Ec), and bulk modulus (Bm). The potential parameters for Al have been taken as a=4.05Å, ε=33.147meV, c=16.399, n=7 and m=6 from Ozgen et al. (2004).

Received 23 August 2012
Available online December 2012

3. Simulation procedure

In this study, the MD method developed by Parrinello & Rahman (1981), which allows anisotropic volume change that can produce a NPH or NPT statistical ensembles, has been used.

In the simulation studies, the equations of motion of the system were numerically solved by using the velocity version of Verlet algorithm. Initial MD cell were constructed on a lattice with face-centered cubic (FCC) unit cell for the systems of 2048 atoms. The periodic boundary conditions were applied on the three dimensions of the MD cell. The temperature of the systems has been controlled by rescaling the atomic velocities at every five integration steps. The simulation processes were carried out as follows:

In order to get an equilibrium liquid state, first, we start at 1000K which is higher than the melting point for Al. At 1000K temperature, it has been observed that the system has a liquid phase and so an extra 100000 steps were waited at 1000K to obtain a relatively mixed liquid phase. Secondly, the liquid phase was cooled down from 1000K to 100K with 50K increment in each run of 10000 steps (21.2×10+15 cooling rate). Third, an extra 40000 steps were waited at 100K to examine the processing of crystallization.

The structures of the systems in solid and liquid phases were examined using the radial distribution function,

$$g(r) = \frac{V}{N^2}\left\langle \frac{\sum_i n_i(r)}{4\pi r^2 \Delta r} \right\rangle \quad (3)$$

Here, g(r) is the probability of finding of an atom in the range between r to $r+\Delta r$, and the angular bracket denotes the time average. N is the number of atoms, ni(r) is the coordination number around atom i in the range from r to $r+\Delta r$.

During each quenching, the structural configurations and atomic positions were recorded at a fixed temperature interval. The structure analysis of crystal, liquid and amorphous states were achieved by RDF. In addition to this, in order to local orientational symmetry of clusters with bond orientational order parameters which are averaged 5 configurations at every temperature was measured.

4. Bond orientational order parameters

The local structures of the atoms in the MD cell are determined from the calculation of the bond orientational order parameters (Steinhardt et al. 1983). In this formalism, the nearest neighbours of each atom in the MD cell, constitute a cluster, and we define the set of neighbours of a particle *i* as all particles *j* that are within a given radius which obtained by using a cut-off distance taken from the minimum of the RDF between the first and the second maximum. The spherical coordinates of each bond in the cluster which are associated with a set of numbers in terms of the spherical harmonics, is calculated from

$$Q_{lm}(\mathbf{r}) \equiv Y_{lm}(\theta(\mathbf{r}), \phi(\mathbf{r})) \quad (4)$$

where Ylm(θ,Φ) are spherical harmonics. We can now characterize the local structure around particle *i* by, and the local bond order parameters can be worked out by averaging Eq. (4) over the number of the bonds (Nb) in the cluster

$$\overline{Q}_{lm}(i) \equiv \frac{1}{N_b(i)} \sum_{i=1}^{N_b(i)} Q_{lm}(\mathbf{r}) \quad (5)$$

where the sum runs over all Nb(i) bonds that particle *i* has with its neighbours. By calculating the average of $\overline{Q}_{lm}(i)$ overall N particles, obtain global orientational order parameters.

$$\overline{Q}_{lm} = \frac{\sum_{i=1}^{N} N_b(i)\,\overline{Q}_{lm}(i)}{\sum_{i=1}^{N} N_b(i)} \quad (6)$$

In order to make the order parameters invariant with respect to rotations of the reference frame, second-order invariants (Ql) and third-order invariants (Wl), respectively, are worked out from the equations below

$$Q_l \equiv \left[\frac{4\pi}{2l+1}\sum_{m=-l}^{l} |\,\overline{Q}_{lm}\,|^2\right]^{1/2} \quad (7)$$

$$W_l \equiv \sum_{\substack{m1,m2,m3 \\ m1+m2+m3=0}} \begin{bmatrix} l & l & l \\ m_1 & m_2 & m_3 \end{bmatrix} \times \overline{Q}_{lm_1}\overline{Q}_{lm_2}\overline{Q}_{lm_3}, \quad (8)$$

where the parameters in square brackets are the Wigner 3j-symbols. The reduced order parameters do not depend strictly on the definition of the nearest neighbours, and can be calculated from:

$$\hat{W}_l \equiv \frac{W_l}{\left[\sum_{m=-l}^{l} |\,\overline{Q}_{lm}\,|^2\right]^{3/2}} \quad (9)$$

which, for a given l is only even so that spherical harmonics are invariant under inversion. The $\hat{W}_l$ parameters are much less sensitive to definitions of the nearest neighbour cut-off than the Q_l parameters. Hence, in the case of bulk systems, it has been seen that as long as the system is in the solid phase, regardless of the degree of local disorder, the $\hat{W}_l$ values are very close to those for a perfect lattice, while in the liquid phase the $\hat{W}_l$ parameters show a wide variance with a mean value of zero. However, the four bond order parameters Q_4, Q_6, $\hat{W}_4$ and $\hat{W}_6$ are generally adequate to identify different crystal structures accurately (Steinhardt et al. 1983).

4. Results and Discussion

Figure 1 shows RDFs change as the temperature falls at different times and the temperatures during the cooling process. At the beginning temperature of 1000 K and the time of 9 ps, the system shows typical features of a liquid structure. It can be seen clearly from the RDF curves that the system behaves as an amorphous phase when the temperature reaches 200 K. The noticeable splitting of the second peak of *g(r)* provides the evidence for an amorphous structure. But, this glass structure is not stable due to the fact that all the RDF peaks become sharper as the temperature decreased. At 100 K temperature and 738 ps, the RDF curves exhibit a characteristic of crystalline peaks at low temperature which indicate the formation of stable crystal-like

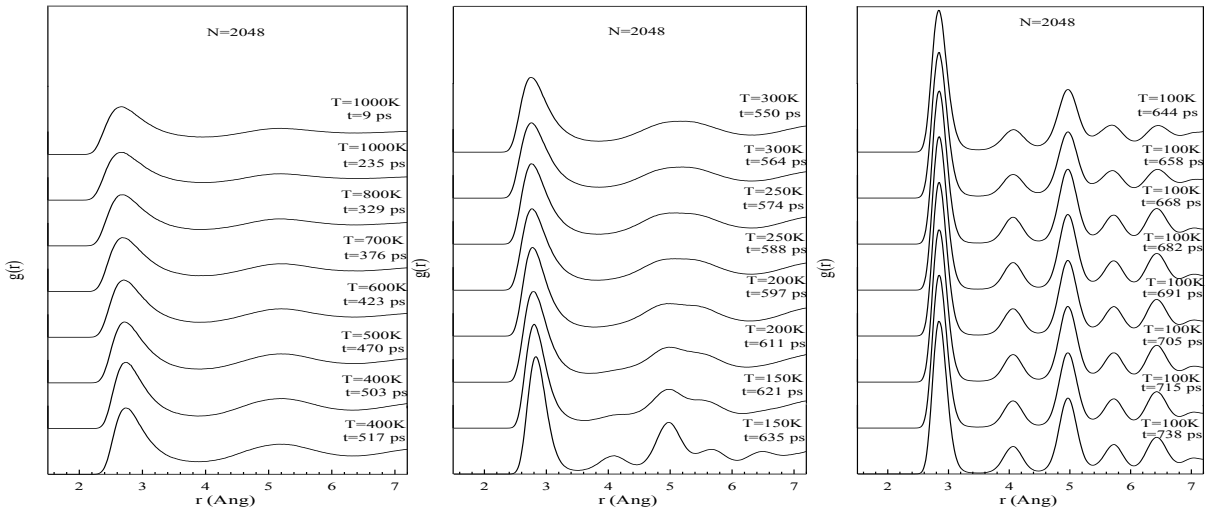

Figure 1. The curves of radial distribution functions at different temperatures during cooling and crystallization process for model system.

ordered clusters. The order degree of the system increased as crystallization began, and in the end a crystalline structure appeared very clearly.

We have focused on investigating the metal clusters, especially of the FCC-like structure, in Al during the transformation and crystallization process from the amorphous state to the crystalline state by using MD simulations based on SCEAM. Bond orientational order parameters for the model system have been calculated from the coordinates of each atom. The coordination polyhedron of an atom is formed by connecting the corners the centres of atoms in the first nearest-neighbour shell with lines. According to this definition, the coordination polyhedra existing in the FCC structure has the shape of cubooctehadron.

Moreover, it is also known that bond orientational order parameters are important parameters to detect the crystalline order, among those, in particular, $\hat{W}_4$ is a sensitive measure of the different cubic orientational symmetries (Steinhardt et al. 1983). The bond orientational order parameters values of atomic clusters are given in Table 1.

Table1. The values of bond order parameters of ideal some typical clusters.

Cluster	Q_6	$\hat{W}_4$
ICOS	0.66332	0
FCC	0.57452	-0.15931
HCP	0.48476	0.13409

As can be seen from Table 1, the order parameters Q_4 and $\hat{W}_4$ are used to distinguish FCC clusters ($Q_4 \geq$ 0.15 and $\hat{W}_4 < 0$) (Wang & Dellago 2003; Gasser et al. 2003). It has been argued by several scholars that the value of Q_6 is a good indicator of the degree of order in the system and it might be used as an order parameter. Indeed, Q_6 is very sensitive to any kind of crystallization and it increases significantly when order appears (Aste et al. 2005; Lechner & Dellago 2008).

Figure 2 presents the global order parameter Q_6 and $\hat{W}_4$ for model system as a function of time during the cooling process. At the time of approximately 600 ps and 200K temperature, which is the beginning of the crystallization, the values of parameters reach stable values implying that the atomic system rearranges from the amorphous phase to ordered crystalline state. In particular, since the values of Q_6 are sensitive to crystallization, the values have increased significantly indicating the order of the crystalline phase. On the other hand, the values of bond orientational order parameters in the Figure 2 approach to the values of FCC given at the crystal phase seen in Table 1. These results show that FCC structures exist are available in the system at 100 K and 738 ps.

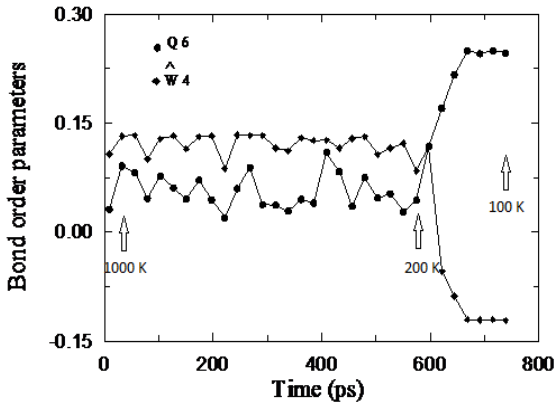

Figure 2. Global order parameters as a function of time during the cooling and crystallization process for the model system.

As can be seen from Table 1, the order parameters Q_6 and $\hat{W}_4$ are of the same order of magnitude for some crystal structures of interest. Especially, Q_6 is used to measure crystal order of the clusters, hence less useful to distinguish different crystal structures, but very useful to act as a generic measure of crystalline state and the symmetry of the crystal clusters. For this reason, the value of Q_6 parameter indicates a transformation from amorphous state to crystalline order.

Figure 3 shows the distributions of Q_4 and $\hat{W}_4$ at the times of 564 ps, 644 ps, 691 ps and 738 ps at different temperatures. As seen in the figure, the system presents distributional properties at the initial states at 300 K and 564 ps, respectively, which represent that the $\hat{W}_4$ parameters show a variation with a mean value of zero since the atoms are randomly distributed in the amorphous phase. On the other hand, Figure 3 presents distributional properties of the system at the times of 691 and 738 ps at 100 K. In the interval of ($Q_4 \geq 0.15$ and $\hat{W}_4 < 0$) representing the FCC clusters, the system has the same distributional properties in the crystal state at 100 K which represent that most parts of their structures contain FCC unit cells.

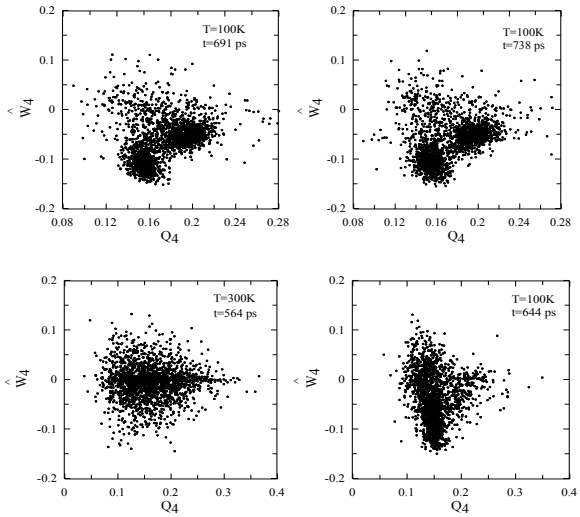

Figure 3. Q_4 and $\hat{W}_4$ distributions for the systems with 2048 atoms at different temperatures during the crystallization process

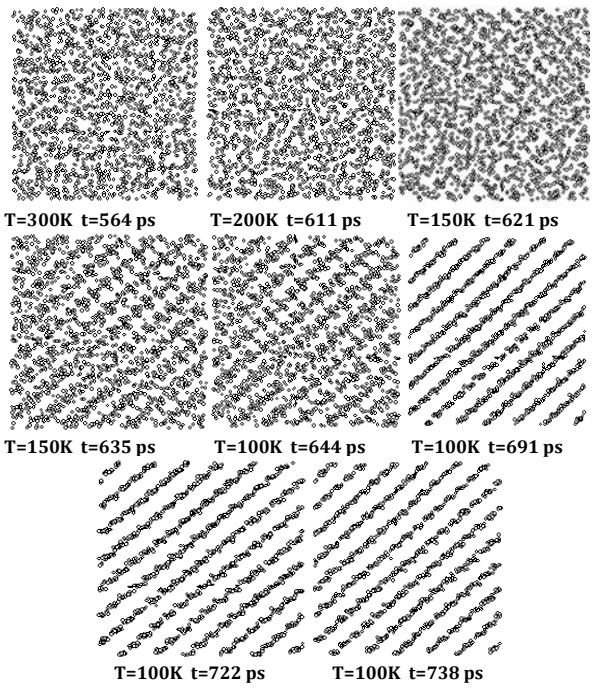

Figure 4. Snapshots of the atomic configuration during the crystallization process of the model Al system.

Figure 4 shows snapshots of atomic configuration at different temperatures during the crystallization process. At the times of 564 ps, 611 ps and 621 ps, the atomic configuration represents an amorphous structure since the atoms are distributed in a disordered way; this picture represents a typical amorphous phase. At the time of 635 ps, the atomic configuration shows the feature of a crystal-like structure due to crystal grains becoming. It can be said from the images that some crystal nuclei have formed in the amorphous phase.
At the time of 738 ps and 100 K, the grain coarsening can be clearly observed as it is obviously seen in the figures that the ordered crystalline structure has almost been formed completely. Namely the crystal embryos have grown forming a stable crystal phase after growth.

5. Conclusion

In this communication, MD simulation calculation, based on the SCEAM method for atomic interactions, was performed on some aluminium systems to determine the local structures from the RDF and the calculation of the bond orientational order parameters. The analysis of the phase transition with these parameters can give us a clear picture of the nucleation of the crystals in the amorphous matrix and the growth of the crystal nuclei. In the calculations we have achieved remarkable results show that the final structures of the systems only consist completely of pure FCC unit cells.

References

Aste T, Saadatfar M, Senden TJ (2005). Geometrical structure of disordered sphere packing. Phys Rev E 71, 061302.

Brown TM, Adams JB (1995). EAM calculations of the thermodynamics of amorphous copper. J Non-Crys Sol 180, 275.

Celik FA, Kazanc S, Yildiz AK, Ozgen S (2008). Pressure effect on the structural properties of amorphous Ag during isothermal annealing. Intermetallics 16, 793-800.

Daw S, Baskes ML (1984). Embedded-atom method: derivation and application to impuries, surfaces and other defects in metals. Phys Rev B 29, 6443-6453.

Desré PJ, Cini E, Vinet B (2001). Homophase-fluctuation-mediated mechanism of nucleation in multicomponent liquid alloys and glass-forming ability. J Non-Crys Sol 288, 210-217.

Erkoc S (1998). Physics of clusters. ARI 51, 11-14.

Gasser U, Schofield A, Weitz, DA (2003). Local order in a supercooled colloidal fluid observed by confocal microscopy. J Phys Condens Matter 15, S375 –S380.

Kazanc S (2007). Molecular dynamics study of pressure effect on crystallization behavior of amorphous CuNi alloy during isothermal annealing. Phys Let A 365, 473-477.

Lechner W, Dellago. C (2008). Accurate determinations of crystal strtuctures based on averaged local bond order parameters. J Chem Phys 129, 114707.

Lu K (1996). Nanocrystalline metals crystallized from amorphous solids: nonocrystallization, structure, and properties. Mater Sci Eng R 16, 161-221.

Nelson DR, Toner J (1981). Bond-orientational order, dislocation loops, and melting of solids and smectic-a liquid crystals. Phys Rev B 24, 363-387.

Ozgen S, Duruk E (2004). Molecular Dynamics Simulation of Solidification Kinetics of Aluminium Using Sutton-Chen Version of EAM. Mater Lett 58, 1071-1075.

Parrinello M, Rahman A (1981). Polymorphic transitions in single crystals: a new molecular dynamics methodi. J Appl Phys 52, 7182.

Pei QX, Lu C, Lee HP (2005). Crystallization of amorphous alloy during isothermal annealing: a molecular dynamics study. J Phys Condens Matter 17, 1493–1504.

Proykova A, Berry RS (2006). Insights into phase transitions from phase changes of clusters. J Phys B: At Mol Opt Phys 39, 167-202.

Schuh CA, Hufnagel TC, Ramamurty U (2007). Mechanical behavior of amorphous alloys. Acta Mater 55, 4067-4109.

Steinhardt PJ, Nelson DR, Ronchetti M (1983). Bond orientational order in liquids and glasses. Phys Rev B 28, 784-804.

Wang Y, Dellago. C (2003). Structural and morphological transitions in gold nanorods: A computer simulation study. J Phys Chem B 107, 9214-9219